Statistical Analysis of Terfenol-D Material Properties

MARCELO J. DAPINO,[1,*] ALISON B. FLATAU[2] AND FREDERICK T. CALKINS[3]

[1]*Department of Mechanical Engineering, The Ohio State University, Suite 224, 650 Ackerman Road, Columbus, OH 43202, USA*

[2]*Department of Aerospace Engineering, University of Maryland, 3184 G.L. Martin Hall, College Park, MD 20742, USA*

[3]*The Boeing Company, P.O. Box 3707 MS 67 ML, Seattle, WA 98124, USA*

ABSTRACT: This article focuses on the characterization of Terfenol-D material properties under magnetic bias, mechanical preloads, AC drive fields, frequencies of operation, and mechanical loads typical of many dynamic transducer applications. These are test conditions unlike those in most Terfenol-D characterization studies. The article also provides an explanation for prior experimental studies which suggest that significant variation in material properties are expected in Terfenol-D elements subjected to repeated tests under fixed operating conditions. Through a statistical framework for the design of experiments and data analysis, we conducted repeatability tests which demonstrate that such variations are likely to be due to imperfect control of the magnetic bias and mechanical preload from test to test, and not to intrinsic material behavior. Frequency response measurements from near DC to past the test transducer's fundamental frequency were combined with classical electroacoustics theory to determine the functional dependence of magnetoelastic properties with respect to varying operating regimes. These properties include two elastic moduli, piezomagnetic coefficient, magnetomechanical coupling coefficient, and two magnetic permeabilities. Analysis of variance (ANOVA) calculations were employed to determine 95% prediction and confidence intervals for the overall material property trends and coefficients of variation associated with the repeatability tests.

Key Words: Terfenol-D, magnetostriction, dynamic measurements, elastic modulus, piezomagnetic coefficient, magnetomechanical coupling, magnetic permeability.

INTRODUCTION

In the last decade, there has been a resurgence of interest in magnetostrictive materials. This is primarily due to the commercial availability of rare earth-iron compounds capable of producing large quasistatic strains of over 1600×10^{-6} in response to moderate magnetic fields of less than 160 kA/m. The most technologically advanced of these compounds is the pseudo binary alloy Terfenol-D, $Tb_{0.3}Dy_{0.7}Fe_{1.9–1.95}$, which has become the primary magnetostrictive material for transducer applications. Terfenol-D exhibits a combination of high single crystal magnetostriction, $\lambda_{111} = 1640 \times 10^{-6}$, and low magnetocrystalline anisotropy, $K_1 = -0.06 \times 10^6$ J m^{-3}. Since magnetostriction is an inherent material property, it does not degrade over time as can be the case with some ferroelectric materials. Thus, Terfenol-D is finding increased use in actuator and sensor applications in which high energy densities and sustained reliability are required. Specifically, Terfenol-D is a suitable material for active vibration control, linear and rotational motion, and acoustic emission in sonic and low ultrasonic regimes (Trémolet, 1993).

Manufacture of high-quality Terfenol-D transducer elements has been perfected to such a degree that it is now possible to obtain in commercial quantities near single crystal material with the ⟨112⟩ crystallographic direction oriented along the drive axis and polycrstalline material produced by ⟨112⟩ directional solidification along the drive axis (Engdahl, 2000). Although the new manufacturing techniques allow for magnetic moment alignment in a direction nearly perpendicular to the drive axis, a static stress or mechanical preload is usually needed in service to induce pre-alignment of the magnetic moments. Magnetostrictive materials with positive magnetostriction, such as Terfenol-D, require compressive preloads along the magnetic drive axis, while tensile stresses are required to prealign magnetic moments in materials such as nickel, which exhibits negative magnetostriction.

In dynamic transducer applications, Terfenol-D is mechanically preloaded and magnetically biased in the manner illustrated in Figure 1, as this enhances the

*Author to whom correspondence should be addressed.
E-mail: dapino.1@osu.edu
Figures 1 and 3 appear in color online: http://jim.sagepub.com

1045-389X/06/07 0587–13 $10.00/0 DOI: 10.1177/1045389X06059500

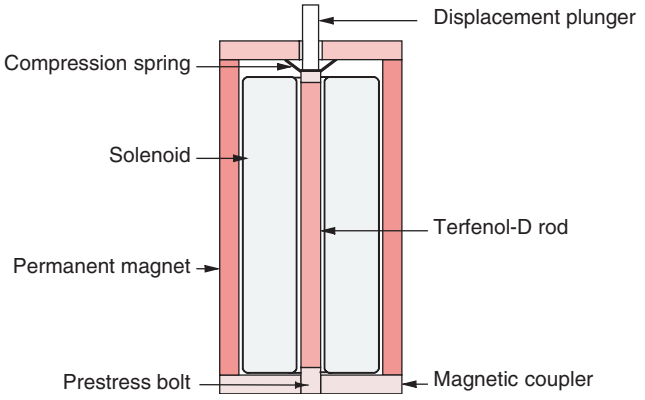

Figure 1. *Terfenol-D transducer employed for dynamic material property characterization. The device is mounted on a large mass to mechanically isolate the transducer dynamics from the testing environment.*

performance and reliability of the material. In this transducer configuration, the stress on the magnetostrictive element can vary substantially as the characteristic σ–ϵ curve of the preload spring is traversed during operation. Furthermore, maximum strain output per field input is achieved at mechanical resonance and properties such as piezomagnetic coefficient, elastic modulus, and magnetic permeability are expected to vary with frequency. This creates conditions unlike those in many material characterization studies in which free standing single crystals are tested with no mechanical preload, unbiased, and at quasistatic frequencies (Clark, et al., 1993).

In Figure 1, a mechanical preload is applied by means of a bolt and cupped spring-washers. In Terfenol-D, due to the magnetomechanical coupling, a sufficiently large compressive stress will shift the preferred orientation of domains to the $\langle 111 \rangle$ axes closest to the plane perpendicular to the drive axis. In that case, the demagnetized length is minimum and the saturation magnetostriction potential is maximum, leading to enhanced magnetostrains. The value of the stress at which this occurs depends on several factors including temperature and composition, but it can be quantified in certain cases as shown in (Dapino et al. 2000). It is noted that mechanically unloaded materials have their magnetic moments aligned randomly, and under the action of a field will only produce about half of the maximum deformation because the moments initially aligned with the drive axis do not contribute to the magnetostriction.

Because magnetostriction is produced by rotation of magnetic moments, a magnetostrictive element driven by an AC field vibrates at twice the drive frequency and its motion is unidirectional. To achieve coherent bidirectional motion, a magnetic bias is applied with a permanent magnet or by passing a DC current through the drive solenoid so that operation takes place around a bias point centered in the steepest region of the M–H and λ–H curves of the magnetostrictive element.

This article is focused on the characterization of Terfenol-D material properties under mechanical loads, magnetic bias fields, AC drive fields and frequencies of operation representative of those encountered in dynamic applications, with a view to quantifying trends and inherent uncertainties in the functional dependence of magnetoelastic properties with respect to varying operating conditions. Knowledge of these trends is essential for high performance design and control of magnetostrictive systems.

The article also focuses on one aspect of Terfenol-D material characterization which has never been adequately addressed. Prior experimental studies have suggested that significant variation in material properties are expected in Terfenol-D elements subjected to repeated tests under seemingly identical transducer conditions (Hall, 1994; Moffett et al., 1991). One question is whether these large variations stem from the stochastic nature of magnetostriction or are due to imperfect control of the various operating variables, especially magnetic bias and mechanical preload. To that end, the article presents a statistical framework for the design of experiments and the evaluation of data collected from Terfenol-D samples subjected to repeated testing under fixed conditions.

Four identical broadband transducers were machined to a tolerance of 0.5 thousandths of an inch. Electrical impedance, electrical admittance, and acceleration per unit current complex functions were measured employing low-signal swept sines at varied applied magnetic field strengths. A total of fifty Terfenol-D samples (thirty solid, and twenty three-laminate) were characterized in randomized performance tests to obtain the material property information. The theoretical framework that provides the material property calculations from measured data was constructed from linear piezomagnetic equations used in combination with canonical transduction equations for electromechanical transducers and a one degree of freedom mechanical model for the test transducers. The study involved three different testing modalities: (i) drive amplitude sensitivity, (ii) test-to-test repeatability, and (iii) mass load sensitivity. The theory employed here is described in the next section, while the experimental methods, results, and pertinent discussion are presented in the subsequent sections.

THEORY

Following classical electroacoustics theory (Hunt, 1982) as applied to Terfenol-D (Calkins and Flatau, 1996), the transduction of energy between voltages and currents (V, I) and forces and velocities (F, v) in a linear electromechanical transducer is modeled by a four-pole mesh as shown in Figure 2. Assuming steady state conditions, i.e. variation with time is expressed as $e^{j\omega t}$,

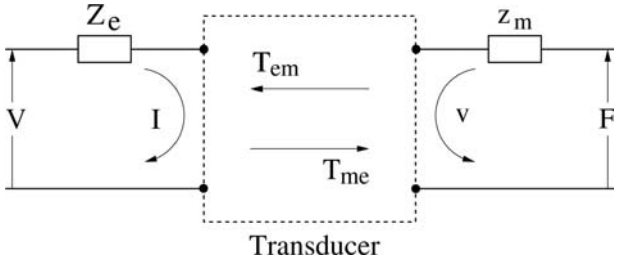

Figure 2. *Schematic representation of an electromechanical transducer.*

the associated linear canonical transduction equations have the form

$$V = Z_e I + T_{em} v \tag{1}$$

$$F = T_{me} I + z_m v \tag{2}$$

where T_{em} and T_{me} respectively denote the transduction terms 'electrical due to mechanical' and 'mechanical due to electrical,' and z_m is mechanical impedance. In the limit when no transduction is present, these two equations reduce to the constitutive formulations for electrical and mechanical systems respectively given by $V = Z_e I$ and $F = z_m v$. Assuming an external load of mechanical impedance z_L, expression (2) for the total output force takes the form

$$-z_L v = T_{me} I + z_m v.$$

Solving for v in this equation gives

$$v = \frac{-T_{me} I}{(z_m + z_L)},$$

which when combined with relation (1) provides an expression for the transducer's electrical impedance frequency response function (FRF)

$$Z_{ee} = \frac{V}{I} = Z_e + \frac{-(T_{em} T_{me})}{z_m + z_L} = Z_e + Z_{mot}. \tag{3}$$

The total electrical impedance FRF is composed of a blocked component Z_e, equal to the ratio between voltage and current that the transducer is prevented from displacing, and a motional impedance Z_{mot} associated with the mechanical motion of the transducer and load. Because Z_{mot} quantifies the electromechanical coupling, it provides a measure of the dynamic properties of the transduction material. The electrical resonance f_r is determined from the principal diameter of the impedance mobility loop in the Nyquist plot of V/I, that is the diameter which intersects the crossover point as shown in Figure 3. In general, this resonance does not correspond to the peak in the magnitude of Z_{ee} due to the phase shift not being exactly zero. Physically, the non-zero phase shift is explained by the presence of energetically dissipative terms in the complex transduction coefficients T_{em} and T_{me}. The two points on the circle at ninety degrees from the

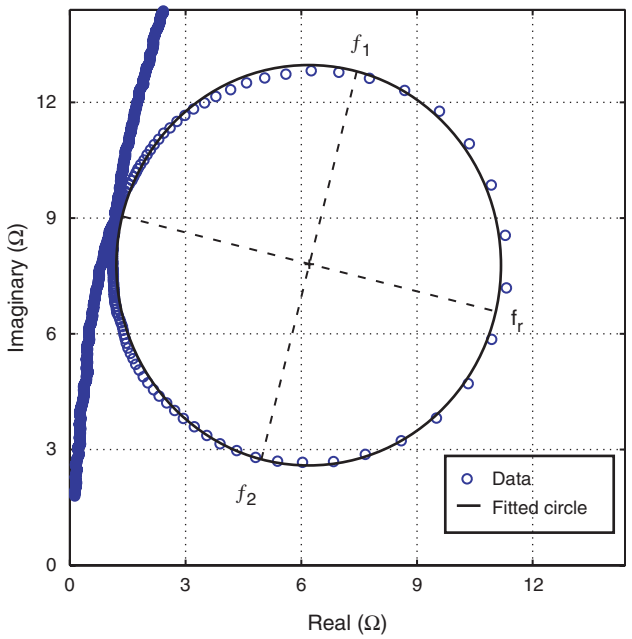

Figure 3. *Nyquist plot of electrical impedance data obtained from a sine sweep excitation. The plot is used for determination of transducer electrical resonance frequency f_r and half power points f_1 and f_2. Each circular point represents one averaged V/I measurement at a fixed frequency. The frequency increases within the circle in the clockwise direction. The computed frequencies are obtained by interpolating the frequencies from two adjacent data points.*

principal diameter are the half power frequencies f_1 and f_2.

In analogous fashion, it has been shown that the electrical admittance FRF has the form (Hunt, 1982)

$$Y_{ee} = \frac{I}{V} = Y_e + \frac{-(T_{em} T_{me}/Z_e^2)}{z_m + z_L + (T_{em} T_{me}/Z_e^2)} = Y_e + Y_{mot}. \tag{4}$$

Since the motional admittance Y_{mot} is not equal to the inverse of Z_{mot}, the information present in the two motional functions is different. One difference between the two functions is that, in the admittance loop, the frequency opposite the crossover point provides a measure of the antiresonance frequency f_{ar}. Similarly, the points on the admittance circle at 90° from the main diameter are the half power points associated with antiresonance, f_{a1} and f_{a2}.

An *effective* magnetomechanical coupling coefficient quantifying the conversion between magnetic and elastic energies in a magnetostrictive transducer can be calculated from the electrical resonant and antiresonant frequencies, and is given by

$$k_{eff}^2 = 1 - \left(\frac{f_r}{f_{ar}}\right)^2. \tag{5}$$

This approach is known as the dynamic method of calculating the magnetomechanical coupling as opposed to the three-parameter method used to directly

determine the *material* coupling coefficient k through formula $k^2 = q^2 E_y^H / \mu^\sigma$, where q is the axial strain (or piezomagnetic) coefficient, E_y^H is the elastic modulus at constant magnetic field and μ^σ is the magnetic permeability at constant stress. The effective coupling coefficient is used to estimate the *material* magnetomechanical coupling coefficient, which is affected by various mechanical stiffnesses and flux linkage, as follows (Hall, 1994)

$$k^2 = \frac{k_{\text{eff}}^2 k_{\text{m}}^H k_{\text{mps}}}{k_M^2 \left(k_{\text{m}}^H + (k_{\text{eff}}^2 k_{\text{mps}} / k_M^2)\right)}. \tag{6}$$

Here, k_{m}^H is the mechanical linear rod stiffness at constant magnetic field, k_{mps} is the mechanical preload stiffness, and k_M is the magnetic flux linkage. The latter parameter has a value of $k_M^2 = 0.9409$ based on finite element calculations by Kvarnsjö (Kvarnsjö, 1993). Because in the transducer of Figure 1 the magnetostrictive element stiffness and the mechanical preload stiffness are arranged as springs in series, the measured transducer resonance frequency f_{r} is related to both stiffnesses through the relationship

$$k_{\text{m}}^H = (2\pi f_{\text{r}})^2 \left(\frac{m_1 m_2}{m_1 + m_2}\right) - k_{\text{mps}} \tag{7}$$

where m_1 is the mass of the transducer base, and m_2 is the effective dynamic mass given by the sum of one-third the mass of the magnetostrictive element and the mass of the transducer load. The resonance frequency is obtained from electrical impedance data as illustrated in Figure 3; the preload stiffness is a transducer parameter to be quantified *a priori*.

The linear rod stiffness is employed to calculate both the elastic modulus at constant magnetic field E_y^H and the piezomagnetic coefficient q. In a one degree of freedom resonator, the elastic modulus is given by

$$E_y^H = \frac{L k_{\text{m}}^H}{\pi A} \tag{8}$$

where A and L respectively denote the cross sectional area and length of the magnetostrictive rod element.

The piezomagnetic coefficient q, which when employing tensorial notation is often denoted d_{33}, provides a measure of linear strain per unit of applied field. In most operating regimes, q is a multivalued map exhibiting hysteresis and nonlinearities. In many commercial dynamic applications in which low preloads are employed to allow for compact drive electronics, the drive field must be kept small to avoid acceleration intensities at resonance that overcome the available preload. In such applications, the strain and magnetization describe Raleigh loops which can be approximated with straight lines through the tips of the loops, therefore allowing one to neglect the effects of nonlinearities and hysteresis. Under these conditions, the piezomagnetic coefficient q can be estimated from the slope of a straight line passing through the tips of the ϵ–H loop. However, a more consistent measure of q can be obtained by recognizing that for a single degree of freedom resonator operated in the stiffness controlled region – defined as frequencies below approximately 10% of the axial fundamental frequency – the displacement per unit force (u/F) has a value equal to the inverse of the axial spring coefficient, or $K = F/u$. By analogy, it has been shown by Hunt (Hunt, 1982) that the average of the strain per unit field in the stiffness controlled region provides a measure of q. Starting with the linearized piezomagnetic equation for the strain,

$$\epsilon = \frac{\sigma}{E_y^H} + qH, \tag{9}$$

recognizing that the force acting on the magnetostrictive rod is equal and opposite to the preload force, $\sigma = -k_{\text{mps}} L / A$, and employing relation (8), the piezomagnetic coefficient takes the form

$$q = \frac{\epsilon}{H}\left(1 + \frac{k_{\text{mps}}}{k_{\text{m}}^H}\right). \tag{10}$$

Assuming that the field is linearly proportional to the drive current, $H = nI$, the piezomagnetic coefficient of a single degree of freedom magnetostrictive resonator becomes

$$q = \frac{u}{nIL}\left(1 + \frac{m_2}{m_1}\right)\left(1 + \frac{k_{\text{mps}}}{k_{\text{m}}^H}\right) \tag{11}$$

where the free-end displacement per unit input current u/I is calculated by averaging in the stiffness controlled region the measured acceleration per unit current divided by the circular frequency squared. Two additional terms with magnitude close to unity are included to account for the effect of transducer masses and stiffnesses which are not otherwise present in a free standing magnetostrictive rod. The mass term $1 + m_2/m_1$ is employed to correct for the fact that the transducer base mass is not infinitely large compared to the moving mass as is the case in an ideal single degree of freedom resonator. The stiffness term corrects for the fact that a small fraction of the magnetostriction is lost to the preload mechanism and is thus unavailable as output work.

To calculate the magnetic permeability at constant stress, the three-parameter method is employed (Clark, 1980)

$$\mu^\sigma = \frac{q^2 E_y^H}{k^2}. \tag{12}$$

Magnetostrictive devices for force control applications are operated at or near their mechanical blocking force, in which the driver is prevented from straining. Under such conditions, the magnetic permeability of the driver decreases relative to μ^σ. This is quantified through the magnetic permeability at constant strain, μ^ϵ.

On the electrical side, a short circuited (electrically blocked) transducer will appear mechanically stiffer; this is quantified through the elastic modulus at constant magnetic induction, E_y^{B}. Clark (Clark 1980) has shown that in low signal regimes the blocked- and open-transducer permeabilities and elastic moduli are related through the magnetoelastic coupling coefficient as follows

$$\mu^{\epsilon} = \mu^{\sigma}(1 - k^2), \tag{13}$$

$$E_y^{\mathrm{B}} = \frac{E_y^H}{1 - k^2}. \tag{14}$$

METHODS

Terfenol-D Material

We analyzed a total of fifty $Tb_{0.3}Dy_{0.7}Fe_{1.9}$ cylindrical rods of nominal dimensions 0.25″ (6.35 mm) diameter by 2.02″ (51.3 mm) length which were manufactured by a Free Standing Zone Melt (FSZM) method. Among the fifty samples, thirty were monolithic rods and twenty were three-laminate rods. Since the manufacturing process employed to grow the crystals yields a range of strain activity for a given nominal composition, the samples were pre-screened according to measured quasistatic strain at 500 Oe (39.79 kA m^{-1}), no magnetic bias, and 1 ksi (6.9 MPa) mechanical prestress, and were assigned one of three classifications. High strain samples exhibited strains of more than 1200×10^{-6}; average strain samples exhibited strains of 1000×10^{-6} to 1200×10^{-6}; and low strain samples exhibited strains of less than 1000×10^{-6}. Ten samples of each rod type were randomly selected for use in this study. Table 1 shows material classification.

Transducer Design

Four identical transducers as shown in Figure 1 were built for this study. Using several units allows to quantify whether the transducers themselves will have statistically significant influence on the determination of Terfenol-D properties. The transducers are broadband laboratory units designed to facilitate accurate material property characterization from dynamic transducer measurements. The transducer base mass is 3 kg and the maximum dynamic load employed in this study is 74.25 g. Because the measured displacement transmissibility ratio between base and load motion is less than 0.01 at the transducer's fundamental frequency, a single degree of freedom resonator model can be accurately used to describe the transducer dynamics.

The Terfenol-D driver is placed inside a solenoid consisting of an innermost single-layered sensing solenoid and a twelve-layer drive solenoid. The solenoid has a nominal length of 2.20″ (56 mm) and is made out of AWG 26 magnet wire. Calibration of the magnetic field intensity per unit current was obtained for each transducer by mapping the field produced along the central axis of the solenoid with a Gauss meter. A slit cylindrical Alnico V permanent magnet surrounds the solenoid and provides most of the required magnetic bias. Fine adjustment of the bias field is achieved by passing a suitable DC current through the drive solenoid.

A bolt located in the transducer's base is used to compress the Terfenol-D rod against two spring washers located in the transducer head. A constant mechanical precompression of 1.0 ksi (6.9 MPa) was used in all tests. This value of the mechanical preload is typical of many dynamic applications as it allows for compact drive electronics. While larger preloads are necessary in high signal applications to avoid unloading of the driver, disproportionally larger fields, and therefore, larger power supplies are required to compensate for such large preloads. Calibration of the spring mechanism on each transducer was obtained using a universal compression machine to relate displacement and force at the transducer output. The measured nominal stiffness of the prestress mechanism is 1.66×10^6 N/m in all transducers. A dial indicator fixture was used prior to assembling each transducer–rod combination to ensure that the position of the prestress bolt was set to obtain a DC displacement in the transducer output corresponding to a 1.0 ksi compressive stress on the driver. The bolt was then locked in position with a locknut.

A magnetic bias H_o was selected for each transducer–rod combination based on the criterion of providing a balanced or symmetric strain-applied field relationship approaching $\pm 500 \times 10^{-6}$ when driving the transducer at magnetic fields of $\pm H_o$ (± 280 Oe nominal) at a quasistatic frequency of 0.7 Hz.

Table 1. Classification of the material employed in this statistical study. All material was manufactured by a Free Standing Zone Melt (FSZM) process.

	Average	Low	High
FSZM – monolithic, 0.25″ × 2.02″	A	B	C
FSZM – three laminate, 0.25″ × 2.02″	D	E	

Experiments

Tests were conducted at AC magnetic field intensities of 2, 5, 10, 20, and 50 Oe (0.16, 0.4, 0.8, 1.6, and 4.0 kA m^{-1}), and loads of four times the nominal mass of the driver (4×), two times (2×), and no load (0×).

The field intensities were selected to range from a low magnetic field to the maximum allowable magnetic field for safe operation at resonance based on the criterion of maintaining the Terfenol-D driver in compression at all times. This is necessary to avoid fracture or chipping of the material. The axial force that produces a 1.0 ksi compressive stress in a quarter inch diameter rod is 218 N (49 lb_f), hence for a total dynamic mass of 74.25 g (corresponding to the 4× loading case), the maximum allowable acceleration is 2922 m/s^2. Our measurements at mechanical resonance (3 kHz) suggest an upper limit of 50 Oe, considering a safety factor of 10% to account for transient effects.

The desired transducer excitation consists of a swept sinusoidal current of constant amplitude from 100 Hz to 5 kHz. Constant current excitation presents challenges as the transducer inductance significantly varies with frequency near resonance. Software programming in the data acquisition system (Tektronix 2642A and 2630) was implemented to vary the voltage supplied to the power supply (Techron 7780 and Techron 7520) used to drive a transducer, such that the actual current flowing through a transducer was constant across the frequency range. The amplifiers were operated in current control mode. The extent to which the amplifiers were able to provide currents that followed the magnitude and phase of the reference drive voltage proved difficult due to high load inductance. To address this, the frequency range was broken into up into twenty spans where the drive current was adjusted in order to obtain a flat current response. In order to establish optimal signal to noise ratios in the various acquired signals, the hardware gain of each channel was set to the minimum value possible that prevents instrument overload. The measured signals include drive coil voltage and current, sensing coil voltage, and output acceleration. The acceleration was measured with a 1.5 g accelerometer. A custom-made summing circuit was used to add the DC and AC drive signals, while operational amplifier circuits were employed to step down the constant current amplifier outputs which monitor drive voltage and current, and to amplify the voltage produced by the sensing coil. In all cases, transducer temperature was held between 20–30°C.

Test Modalities

The material characterization study comprises the following three distinct test modalities:

(i) Drive amplitude sensitivity. Trends in magnetoelastic properties of Terfenol-D under varied applied fields are investigated for all fifty samples. From these trends, functional relations are developed employing Analysis of Variance (ANOVA) analysis. In these 'baseline' tests, a mass load equal to four times the nominal mass of the rod, which has a value of 15 g, was used. Sinusoidal zero to peak AC drive field amplitudes of 2, 5, 10, 20, and 50 Oe (0.16, 0.4, 0.8, and 4 kA m^{-1}) were used to excite the transducer. The experimental matrices, which are balanced with respect to transducers (except for rod type A), were assembled by random assignment of the four transducers to each rod/field intensity combination. Blocks of fifty rod/transducer assemblies and measurements for each rod type were run sequentially for rod types A through E.

(ii) Repeatability tests. While the baseline study was designed to observe variations in measurements in different rod/transducer combinations under varied AC drive field intensities and fixed mass loading, the repeatability study is focused on quantifying the variation in measurements taken at a fixed drive field amplitude in an assembled rod/transducer pair. This variation is referred to as the sampling error. Rod/transducer pairs were assembled and cycled through 8–10 consecutive test repetitions at a fixed drive field intensity before proceeding to assemble and test the next set of rod/transducer/drive field combination. Among type-A rods, three samples were selected as best, average, and worst in terms of quasistatic maximum strain. Tests with a load of 60 g were repeated ten times at AC drive fields of 5, 10, 20, and 50 Oe. These procedures underwent a slight revision for the rod types B through E. Four samples were used instead (worst, best, and two average performing based on quasistatic maximum strain), for a total of sixteen rod/drive field combinations per rod type. The four transducers were assigned to each rod/drive field combination in a Latin Square fashion. Each measurement was repeated eight times. Rod/transducer combinations were fixed for a set of three mass load tests. Blocks of sixteen sets of measurements (twelve for rod type A) were run sequentially for rod types A through E.

(iii) Mass load sensitivity. Information on variation of properties with transducer load was obtained using for each rod type the best, worst, and two average performing rods in terms of quasistatic maximum strain. As in the repeatability study, only three rod type A samples were tested. The three loading conditions employed include four times the nominal mass of the rod (60 g), twice the nominal mass of the rod (30 g), and no load (accelerometer mass only, ≈1.5 g). Drive amplitudes of 5, 10, 20, and 50 Oe were employed, and transducers were assigned in a similar fashion as in the repeatability study. Blocks of sixteen measurements (twelve for rod type A) were run sequentially for rod types A through E.

Statistical Analysis

Three main factors were controlled in the baseline and repeatability studies: rods, transducers, and AC drive

fields. The external mass is an additional test factor in the mass load sensitivity study only. Other operating parameters such as magnetic bias, mechanical prestress, and transducer temperature were kept constant following the above-mentioned criteria.

The effects of factors were identified by performing an ANOVA to each of the material properties. Each rod type was assigned its own experimental matrix. Except for rod type A, transducers were assigned to rod/drive field combinations in a balanced fashion, i.e., each transducer was used in the same number of tests within a rod type, but each experimental matrix was unbalanced. A completely balanced experimental matrix would have $(t \times r \times d)$ elements corresponding to t transducers, r rods and d drive levels. The matrices used in this study are $(1 \times r \times d)$-dimensional.

The experiment is therefore unbalanced with respect to all factors considered together, implying that on these measurements, type III sums of squares are being performed instead of the usual types I and II (Rawlings, 1988; SAS/STAT, 1990). The group of ten samples in each rod type constitute a random sample from the population of like rods. The effects of rods are thus random, which allows the extrapolation of results from the random sample to the whole population of similar rods. On the other hand, the effects of transducers and drive field intensities are treated as fixed.

A statistical model was constructed which, upon ignoring factor interactions, has the general form

$$Y_{ijk} = \tau_i + \rho_j + f(H_k) + \varepsilon_{ijk}$$

where τ_i represents the fixed effect of the ith transducer, ρ_j represents the random effect of the jth rod, $f(H_k)$ represents the functional dependence of Y on drive field H_k and ε_{ijk} is a random component attributed to experimental error. Depending on the relative significance of rods and transducers within the model in each particular case, these effects may be dropped from the model either individually or simultaneously. We assume that ρ_j is independently and identically distributed (iid) normal with mean 0 and variance σ_ρ^2; ε_{ijk} is assumed iid normal with mean 0 and variance σ^2. Since rods have a random contribution to the measurements, the variance of the model is $Var(Y) = \sigma_\rho^2 + \sigma^2$. Confidence and prediction intervals are computed from the reduced model in which the effect of rods and transducers are assumed to have no statistical significance.

RESULTS AND DISCUSSION

It was shown through model equations (1)–(14) that four material properties fully define the magnetoelastic behavior of magnetostrictive materials when they are employed in a transducer environment consisting of a magnetic circuit, which is used to generate a suitable magnetic bias while minimizing overall flux leakage, and a mechanical path which provides a moderate preload of 1 ksi. The four properties considered in this statistical analysis are the elastic modulus at constant applied field, E_y^H, piezomagnetic coefficient, q, magnetomechanical coupling, k, and permeability at constant strain, μ^ϵ. The remaining properties can be calculated from these.

Baseline Study

Data from the laminated average material (type-D rods) will be used to demonstrate the procedures followed for obtaining material property information from experimental data. Evaluation of elastic modulus at constant applied field as a function of applied field data in Figure 4 suggests that a quadratic model is appropriate to fit the measurements. Letting $\mu(H)$ be the mean response at drive field H, a possible model for the mean values is

$$\frac{\mu(H)}{10^9} = \beta_0 + \beta_1 \log(H) + \beta_2[\log(H)]^2$$

where β_i are the coefficients of the second-order logarithmic model. The approximately constant spread allows fitting the model to the data by the least squares method, which yields

$$\frac{\hat{\mu}(H)}{10^9} = 57.01 - 3.71 \log(H) - 4.48[\log(H)]^2.$$

The mean response is also included in Figure 4, together with 95% confidence and prediction intervals computed from the standard error of the least squares fit. There is 95% confidence that the average elastic modulus of type-D material will lie within the region delimited by the confidence interval lines. Similarly, 95 out of 100 times, the elastic modulus of any individual type-D rod will lie

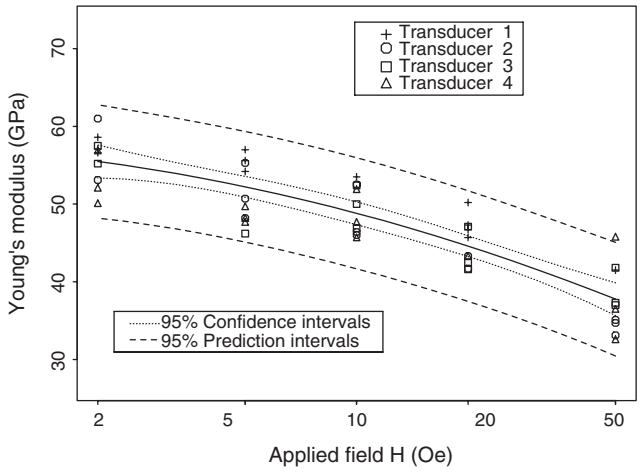

Figure 4. *Baseline study: elastic modulus at constant applied field, E_y^H. Rod type D experimental data, estimated means (solid line), and 95% confidence and prediction intervals.*

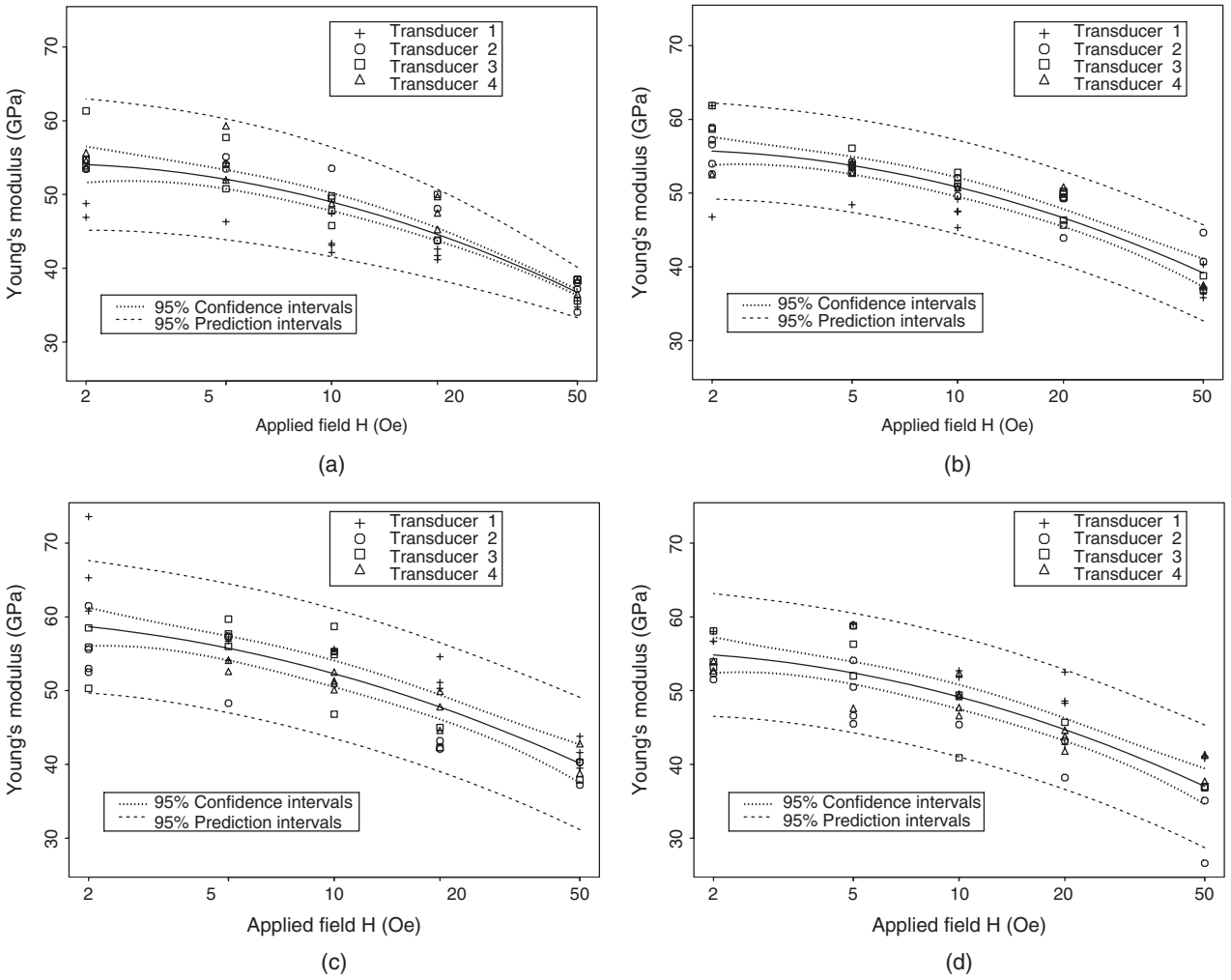

Figure 5. *Baseline study: elastic modulus at constant applied field experimental data by transducer, estimated means, and 95% confidence and prediction intervals. Panels (a) through (d) respectively show rod types A, B, C, and E.*

within the region delimited by the two prediction interval lines.

Figure 5 shows the elastic modulus experimental data and fitted curves for rod types A, B, C, and E. The measurements show a softening with increasing AC field that is uniform across rod types and which is consistent with lattice behavior observed in prior quasistatic measurements (Clark et al., 1993). The scatter of the data or error bar is homogeneous for all rod types except rod type A, which shows a statistically significant decrease in the scatter with increasing AC fields. Despite the fact that transducers were designed with accurate tolerances, the scatter in the data is significant across rod types and throughout the range of field intensities being considered.

The predicted mean responses are compared for all rod types in Figure 6. A decreasing, quadratic relationship is observed in all cases. High quasistatic strain samples (type-C material) consistently show the highest elastic modulus across the applied field range. This result is unexpected considering that, from a quasistatic point of view, larger magnetostrictions are usually associated with softer alloys and underscores the difference between conventional quasistatic material property characterization and the dynamic approach

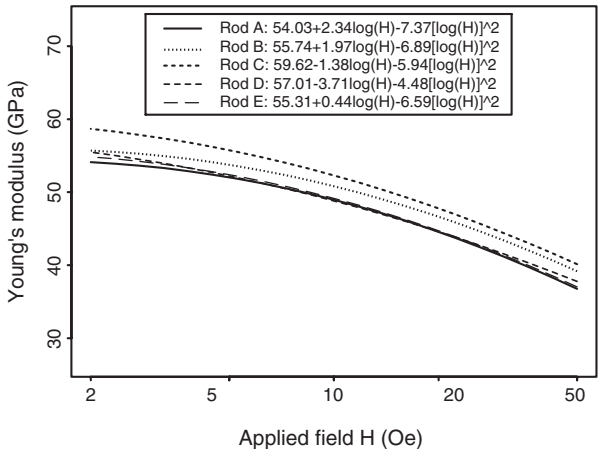

Figure 6. *Baseline study: fitted mean curves of elastic modulus at constant applied field, E_y^H, by rod type.*

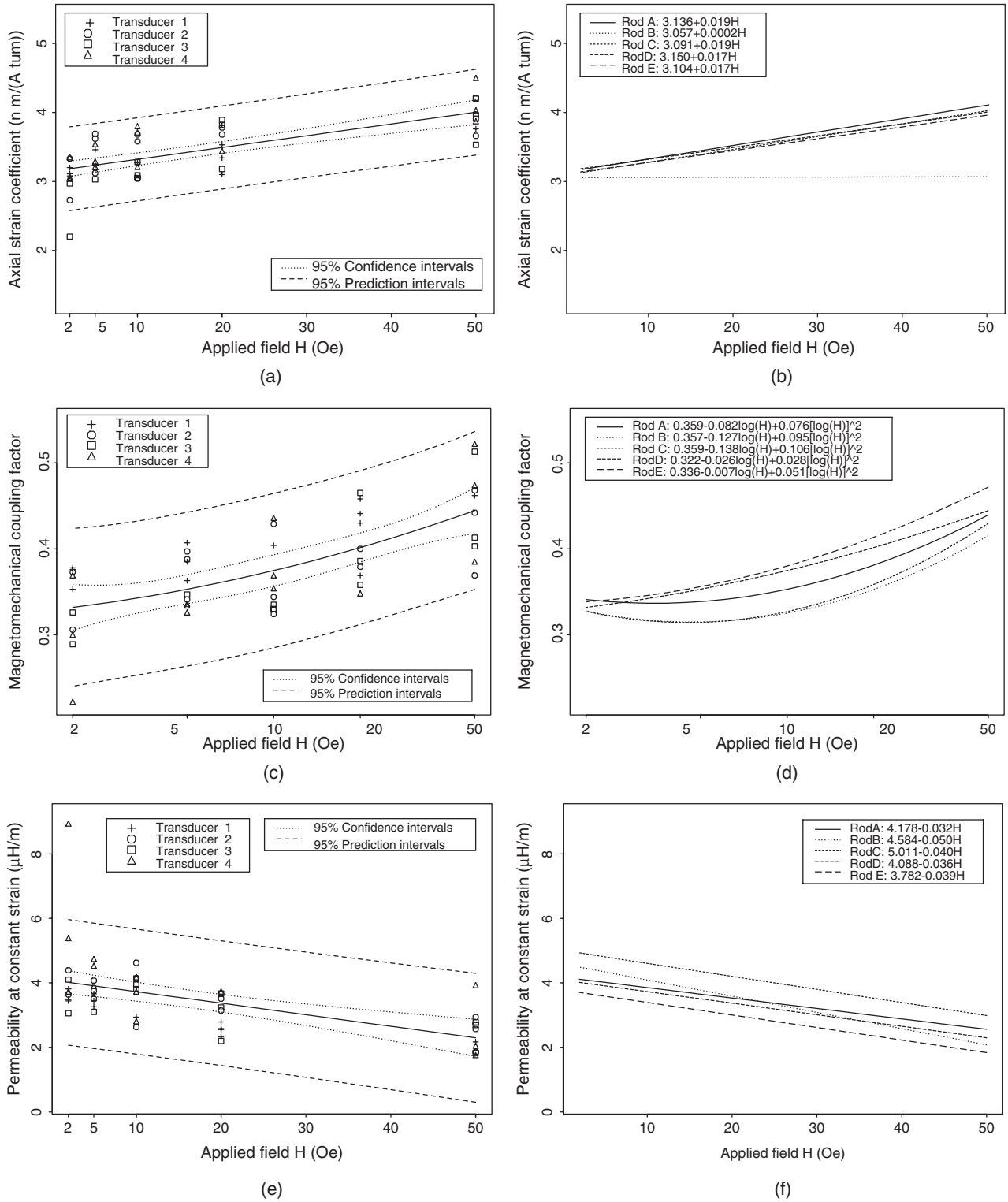

Figure 7. *Baseline study. From top to bottom: piezomagnetic coefficient, q, magnetomechanical coupling factor, k, and permeability at constant strain, μ^{ϵ}. Left column: type-D material experimental data, mean response, and 95% confidence and prediction intervals. Right column: fitted means for rod types A through E.*

employed in this study. The observed decrease in apparent modulus with increasing AC field intensity is consistent with results presented by Calkins (Calkins, 1997). This effect is unlike the ΔE effect, whereby the elastic modulus of unbiased Terfenol-D first decreases and then increases with increasing DC field.

Figure 7 shows experimental data and fitted curves for piezomagnetic coefficient, magnetomechanical

coupling factor, and permeability at constant strain. In order to assess the spread in the measurements at each drive field intensity, the mean square of the error (MSE) in the regression model is compared among material types for each property in Table 2. Since MSE is an estimator of the variance σ^2, a small value of the MSE indicates small spreads in the measurements, whereas a large MSE suggests large spreads. The coefficient of determination R^2 is often used to judge the adequacy of a regression model (Myers, 1990) and is also included in Table 2. The degrees of freedom left for error are provided as well.

Repeatability Study

Elastic modulus at constant field repeatability data of four rod type D samples is presented in Figure 8. Each group of data points represents eight repeated tests in one of the four transducers as indicated in the figure legend. Note that the scatter observed in the repeatability results does encompass the prediction intervals estimated from the baseline type-D material study.

One parameter that quantifies relative uniformity in a given set of repetitions is the coefficient of variation, which is defined as

$$cv = 100\% \times \frac{\sigma}{\mu}$$

where σ is the standard deviation and μ is the mean value of the measurements. The smaller the coefficient of variation, the more 'repeatable' a measurement is said to be. The coefficients of variation range approximately between 0.44 and 4.55% in this particular case. Table 3 summarizes the calculations of means ($\bar{x}$), standard deviations (σ), and coefficients of variation (cv) for the

Table 2. Baseline study: mean square of error (MSE), coefficient of determination (R^2), and degrees of freedom of error (df) in the regression models. Asterisks indicate weighted least squares fits.

	E_y^H			q			k			μ^ϵ		
Rod type	**MSE**	**R^2 (%)**	**df**	**MSE**	**R^2 (%)**	**df**	**MSE**	**R^2 (%)**	**df**	**MSE**	**R^2 (%)**	**df**
A	19.598*	85.80*	47*	0.0148	44.68	48	0.0016	48.67	47	0.3484	48.65	48
B	9.61	79.25	47	0.341*	48.64*	48*	0.0011	55.92	47	2.8708*	47.43*	48*
C	18.22	71.21	47	0.362	23.26	48	0.010	64.49	47	0.7207	41.78	48
D	12.07	77.08	47	0.088	51.18	48	0.0019	46.19	47	0.9063	30.90	48
E	15.67	72.87	47	0.198	31.84	48	0.011	67.91	47	0.3644	56.70	48

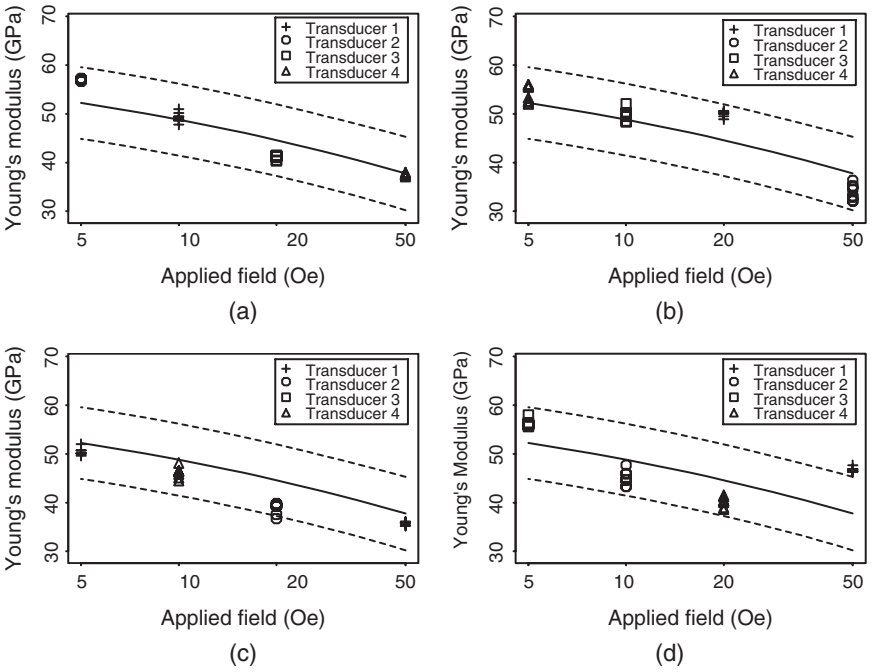

Figure 8. *Repeatability study: rod type D elastic modulus at constant applied field experimental data, sorted by rod. (a) Rod #3, (b) rod #6, (c) rod #7, and (d) rod #9. The solid and dashed lines respectively represent estimated means and 95% prediction intervals computed from the baseline data (see Figure 4).*

Table 3. Repeatability study: type-D material summary statistics for elastic modulus at constant applied field, by rod and by drive field intensity. Column 'Tr' denotes the transducer employed in each set of repetitions.

	Rod #3				Rod #6				Rod #7				Rod #9			
Drive level	$\bar{x}$	σ	**cv%**	**Tr**	$\bar{x}$	σ	**cv%**	**Tr**	$\bar{x}$	σ	**cv%**	**Tr**	$\bar{x}$	σ	**cv%**	**Tr**
5	56.938	0.250	0.44	2	54.175	1.753	3.24	4	50.425	0.732	1.45	1	56.250	0.741	1.32	3
10	49.288	0.988	2.00	1	49.725	1.174	2.36	3	46.129	1.159	2.51	4	45.025	1.474	3.27	2
20	41.112	0.455	1.11	3	50.000	0.558	1.12	1	38.888	1.117	2.87	2	40.163	0.984	2.45	1
50	37.503	0.245	0.65	4	33.925	1.542	4.55	2	35.725	0.320	0.90	1	46.725	0.462	0.99	4
Average	46.225	0.561	1.05		46.956	1.313	2.82		41.679	0.758	1.93		47.041	0.971	2.01	

rod type D data at magnetic fields ranging from 5–50 Oe. Average coefficients of variation of individual samples range between 1 and 2.8%, as shown in the bottom row. The average coefficient of variation of the four rods (overall mean cv of the lot) is used for comparison between rod types. It is noted that the average coefficient of variation for each rod (average cv) is not equal to the pooled standard deviation divided by the mean, or the average of σ divided by the average of $\bar{x}$. The average of the coefficients of variation gives, in this case, a better estimation of the expected repeatability. For this particular rod type, the average coefficient of variation of the lot is $cv = 1.95\%$. Table 4 compares coefficients of variation for all rod types, sorted by property.

Type-A rods consistently have larger sampling errors for all properties, possibly due to operator influence, since type A material was tested first in this twelve month study. A second factor is that a faulty accelerometer was responsible for higher than expected coefficients of variation in q and μ^{ϵ}. Despite these external factors having statistical effect on the results, the measurements reveal that no fundamental differences are evident among rod types, either among all five rod types considered individually or between solid and three-laminate material. The coefficients of variation are, in most cases, smaller than $\approx 5\%$. This result suggests excellent repeatability in the properties of commercial Terfenol-D material, well within the experimental error. Prior studies have suggested much larger variations which we do not attribute to the material being inconsistent, but to inaccurate control of external factors such as mechanical preload and magnetic bias. The high sensitivity of Terfenol-D properties to these factors has been substantiated in a prior study (Calkins et al., 1997).

Comparing coefficients of variation among properties, the elastic modulus was less variable than the other three material properties under study. On the other hand, the permeability at constant strain exhibits the highest coefficients of variation. This is not altogether unexpected because, unlike the other properties, calculation of permeability values from data involves three different sets of measurements, namely acceleration, input voltage, and input current functions. It is therefore concluded that the propagation of error from the three measurements led to increased sampling errors and hence, higher coefficients of variation in the calculation of μ^{ϵ}.

Table 4. Repeatability study: average coefficients of variation % by rod type and by property. Asterisks indicate data affected by a faulty accelerometer.

	Property			
Rod type	E_y^H	q	k	μ^{ϵ}
A	1.75	4.57*	3.48	11.69*
B	0.74	0.96	1.92	5.15
C	0.72	2.14	1.82	4.88
D	1.95	2.13	1.99	5.72
E	1.71	1.91	1.79	5.66

Mass Load Sensitivity Study

A modified statistical model is assumed in which a given combination of transducer, drive field intensity, and Terfenol-D sample is treated as a fixed block within which each of the three loading cases ($4\times$, $2\times$, and $0\times$) is applied once. The following model is assumed

$$Y_{ijk} = \mu + \rho_i + \beta_{ij} + \lambda_k + (\rho\lambda)_{ik} + \varepsilon_{ijk} \qquad (15)$$

where Y_{ijk} is the observation under the ith rod type, jth block (transducer/field/rod combination) and kth loading case; ρ_i is the main effect of the ith rod type; β_{ij} is the main effect of the jth block nested in the ith rod type; λ_k is the main effect of the kth loading case; $(\rho\lambda)_{ik}$ is the interaction between the ith rod type and the kth loading case; and ε_{ijk} is a random term due to experimental error. Significant factors and interactions are identified from ANOVA calculations and F-tests based on type III sums of squares. Nominal differences among estimated means corresponding to each loading case are investigated by computing 95% Bonferroni intervals (Snedecor and Cochran, 1989) which provide an adjustment for multiplicity.

Mean curves were fitted using model equation (15). The mean curves for E_y^H are illustrated in the conditioning plot of Figure 9, which also shows experimental data and confidence intervals. For a load

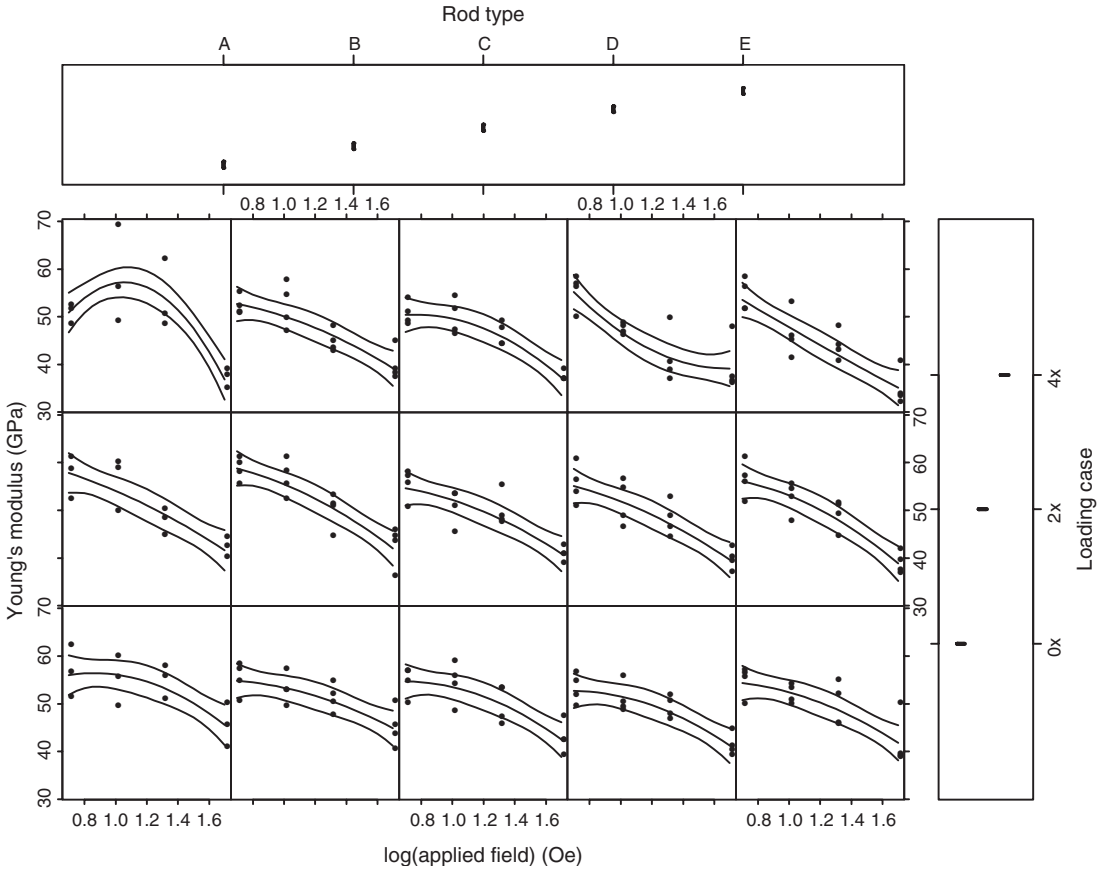

Figure 9. *Mass load sensitivity study: conditioning plot of elastic modulus at constant applied field, E_y^H, by rod type.*

equal to four times the mass of the sample (4×), for all four rod types cases, most experimental data points lie within the prediction intervals computed in the baseline study. However, for type A rods, the fitted curves do not agree with the trends seen in Figures 4 and 5. The trends in the 0× and 2× loading cases do agree with the results observed in the baseline study in terms of the shapes observed in the fitted curves. For this range of loads, the effect of loading on the elastic modulus is statistically small.

CONCLUSIONS

The importance of gathering Terfenol-D material property information in a transducer environment was discussed. Functional expressions of four Terfenol-D material properties (E_y^H, q, k, and μ^ϵ) as a function of applied AC magnetic fields up to 50 Oe were developed. By using statistics principles, 95% prediction and confidence intervals were calculated. These intervals provide formal assessment of the experimental error under varied applied fields and controlled transducer parameters.

The ability to reproduce measurements in Terfenol-D transducers was studied. Results obtained by assessment of coefficients of variation to repeated measurements under fixed drive levels and controlled transducer conditions demonstrate that in most cases, the measured coefficients of variation are smaller than $\approx$5%.

Finally, the sensitivity of Terfenol-D transducers to load changes was investigated. The results additionally emphasize the importance of adequate sampling in Terfenol-D transducer studies, and provided preliminary insight on variation of material properties under varied loads.

ACKNOWLEDGMENTS

The authors wish to acknowledge Francis Pascual and the numerous undergraduate students who helped in data collection. Financial support for M.J.D. was provided in part by Ohio State University. Support for A.B.F. and M.J.D. was provided by NSF Young Investigator Award #CMS-94-57288 and ETREMA Products, Inc. through Iowa State University IPRT Contract #95-05. Support for F.T.C. was provided by a NASA graduate research fellowship of the Structural Acoustics Branch of NASA Langley.

REFERENCES

Calkins, F.T. and Flatau, A.B. 1996. "Transducer Based Measurements of Terfenol-D Material Properties," In: *Proceedings of SPIE Smart Structures and Materials*, Vol. 2717, San Diego, CA, pp. 709–719.

Calkins, F.T. 1997. "Design, Analysis and Modeling of Giant Magnetostrictive Transducers," PhD Dissertation, Iowa State University, Ames, Iowa.

Calkins, F.T., Dapino, M.J. and Flatau, A.B. 1997. "Effect of Prestress on the Dynamic Performance of a Terfenol-D Transducer," *Proceedings of SPIE Smart Structures and Materials*, Vol. 3041, San Diego, CA, pp. 293–304.

Clark, A.E. 1980. "Magnetostrictive Rare Earth-Fe_2 Compounds," Wolfarth, E.P. (ed.), *Ferromagnetic Materials*, Vol. 1, North Holland Publishing Co.

Clark, A.E., Restorff, J.B. and Wun-Fogle, M. 1993. "Magnetoelastic Coupling and ΔE Effect in (Tb_xDy_{1-x}) Single Crystals," *J. Appl. Phys.*, 73(10):6150–6152.

Dapino, M.J., Smith, R.C. and Flatau, A.B. 2000. "Structural-magnetic Strain Model for Magnetostrictive Transducers," *IEEE Transactions on Magnetics*, 36(3):545–556.

Engdahl, G. (ed.) 2000. "Handbook of Giant Magnetostrictive Materials," Academic Press, San Diego, CA.

Hall, D.L. 1994. "Dynamics and Vibrations of Magnetostrictive Transducers," PhD Dissertation, Iowa State University, Ames, IA.

Hunt, F.V. 1982. *Electroacoustics: The Analysis of Transduction, and its Historical Background*, American Institute of Physics for the Acoustical Society of America.

Kvarnsjö, L. 1993. "On Characterization, Modelling and Application of Highly Magnetostrictive Materials," PhD Dissertation, Royal Institute of Technology, Stockholm, Sweden.

Moffett, M.B., Clark, A.E., Wun-Fogle, M., Linberg, J., Teter, J.P. and McLaughlin, E.A. 1991. "Characterization of Terfenol-D for Magnetostrictive Transducers," *J. Acoust. Soc. Am.*, 89(3):1448–1455.

Myers, R.H. 1990. *Classical and Modern Regression with Applications*, PWS-Kent Publishing, Co., Boston, MA.

Rawlings, J.O. 1988. *Applied Regression Analysis: A Research Tool*, Wadsworth, Inc., Belmont, CA.

SAS/STAT User's Guide, Volume 2. 1990. Version 6, 4th edn., SAS Institute, ISBN 1-55544-376-1.

Snedecor, G.W. and Cochran, W.G. 1989. *Statistical Methods*, Iowa State University Press, Ames, IA.

Trémolet de Lacheisserie, E. 1993. "Magnetostriction Theory and Applications of Magnetoelasticity," CRC Press, Inc., Boca Raton, FL.